ChemPubSoc Europe
DOI: 10.1002/chem.201501671
CHEMISTRY A European Journal Communication

Solar Cells

Enhanced Photocatalytic Reduction of CO_2 to CO through TiO_2 Passivation of InP in Ionic Liquids

Guangtong Zeng,[a] Jing Qiu,[b] Bingya Hou,[c] Haotian Shi,[a] Yongjing Lin,[d] Mark Hettick,[d] Ali Javey,[d] and Stephen B. Cronin*[a, c]

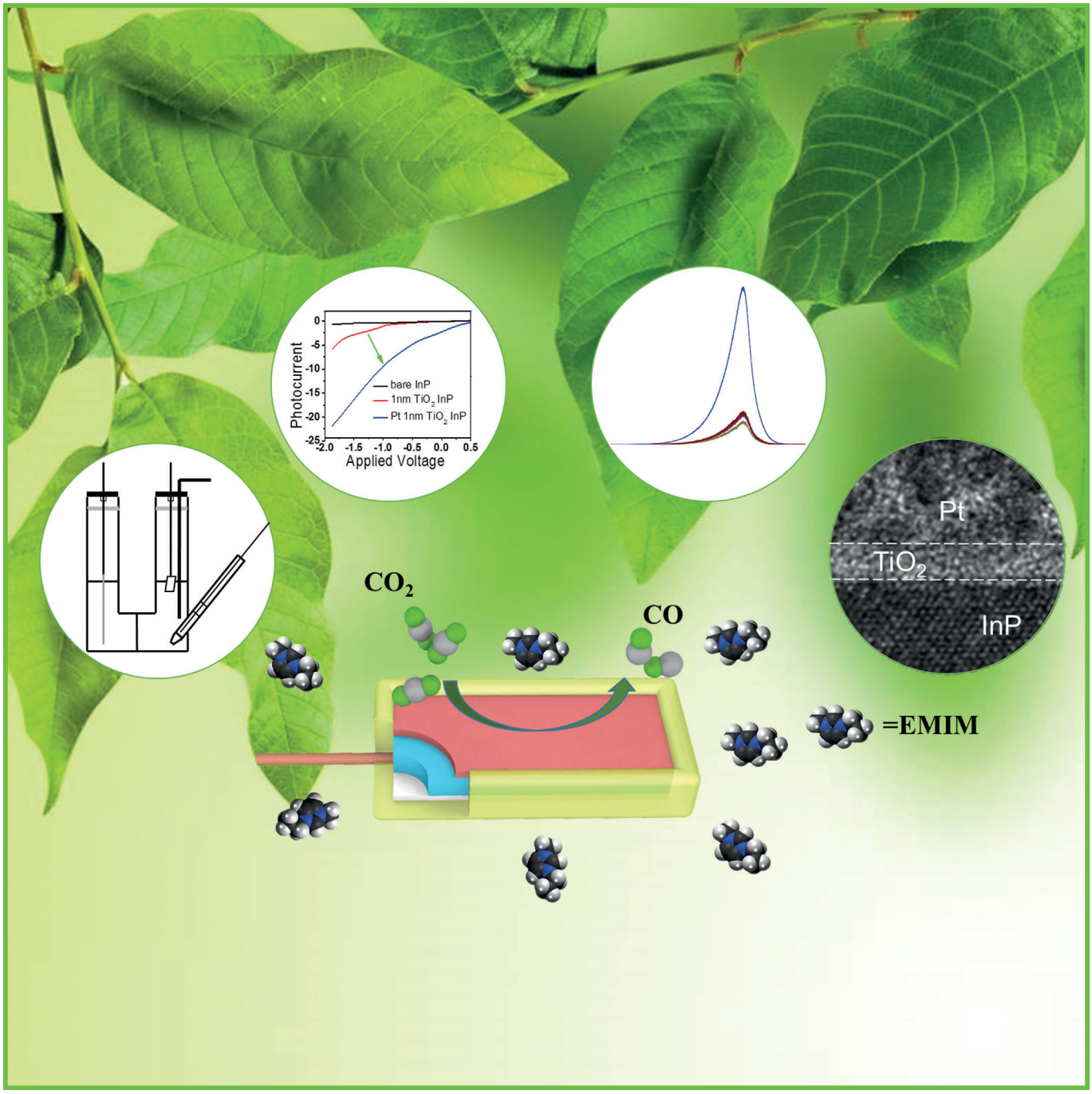

Abstract: A robust and reliable method for improving the photocatalytic performance of InP, which is one of the best known materials for solar photoconversion (i.e., solar cells). In this article, we report substantial improvements (up to 18×) in the photocatalytic yields for CO_2 reduction to CO through the surface passivation of InP with TiO_2 deposited by atomic layer deposition (ALD). Here, the main mechanisms of enhancement are the introduction of catalytically active sites and the formation of a *pn*-junction. Photoelectrochemical reactions were carried out in a nonaqueous solution consisting of ionic liquid, 1-ethyl-3-methylimidazolium tetrafluoroborate ([EMIM]BF_4), dissolved in acetonitrile, which enables CO_2 reduction with a Faradaic efficiency of 99% at an underpotential of +0.78 V. While the photocatalytic yield increases with the addition of the TiO_2 layer, a corresponding drop in the photoluminescence intensity indicates the presence of catalytically active sites, which cause an increase in the electron-hole pair recombination rate. NMR spectra show that the $[EMIM]^+$ ions in solution form an intermediate complex with CO_2^-, thus lowering the energy barrier of this reaction.

Photocatalytic reduction of CO_2 is an exciting reaction system with the ability to convert an abundant greenhouse gas to combustible hydrocarbon fuels using sunlight.[1] The direct conversion of solar energy into chemical bonds that can later be released in a carbon neutral cycle has several advantages over solar-to-electric energy conversion, most notably, the ability to store large amounts of energy (~GW).[2] CO_2 is recognized as a naturally abundant and inexpensive carbon source for the production of organic fuels.[3] The two electron reduction of CO_2 to CO (i.e., $CO_2 + 2e^- + 2H^+ \rightarrow CO + H_2O$) is an important reaction, since CO can react with water to generate hydrogen gas, and this CO/H_2 mixture (syngas) can subsequently be used to produce synthetic petroleum using the Fischer–Tropsch process.[4] Many attempts have been made to reduce CO_2 by $2e^-$ processes to various species such as CO and formic acid, as reported in previous literature.[1a,b,5] The most likely first step in these multi-electron reactions is the one-electron reduction to the CO_2^- intermediate,[6] which lies 1.7 eV above the conduction band of TiO_2 and 1.6 eV above InP, as first proposed by Bockris et al.[7] Since then, others have also attributed the high overpotentials required to drive this reaction to the formation of the CO_2^- intermediate.[2c,i,8] Recently, some researchers have attempted to reduce CO_2 into CO in ionic liquids (ILs).[9] In an aqueous system, Rosen et al. reported an effective electrocatalytic system that reduces CO_2 to CO using an ionic liquid 1-ethyl-3-methylimidazolium tetrafluoroborate ([EMIM]BF_4) to lower the energy of the CO_2^- intermediate.[10] In a non-aqueous solution, Sun et al. used a similar ionic liquid 1-ethyl-3-methylimidazolium bis(trifluoromethylsulfonyl)imide [EMIM][Tf_2N] dissolved in acetonitrile for the electrochemical reduction of CO_2, which resulted in a 0.18 V reduction in the overpotential required to drive this reaction.[11] Also, Rosenthal's group reported a Bi-based electrocatalyst demonstrating highly selective conversion of CO_2 to CO with a 0.195 V overpotential.[12] Metal co-catalysts, such as Pt are known to play an important role in the semiconductor-based photocatalytic systems.[13] Xie's group reported a Pt-promoted TiO_2 photocatalyst under UV illumination with enhanced selectivity for CO_2 reduction.[14]

Recently, we have observed the photoreduction of CO_2 to methanol in an aqueous solution on bare GaP and TiO_2-passivated GaP.[3] In addition to providing a stable photocatalytic surface, the TiO_2-passivation layer improves the photocatalytic efficiency and lowers the overpotential required to drive this reaction.[3,15] However, GaP's indirect band gap results in a particularly low absorption coefficient, which is disadvantageous for photocatalysis and results in a low overall photoconversion efficiency. Also, a particularly low Faradaic efficiency was observed due to the formation of H_2. InP, on the other hand, is a direct band gap semiconductor and an excellent candidate for solar photocatalysis. The record high solar-to-hydrogen efficiency of 13.3% was demonstrated in 1982 by using a system that employed *p*-type InP photocathodes covered with Pt catalysts.[16] More recently, Lee et al. reported 14% efficient water splitting using InP nanopillars with a Ru catalyst.[17] However, photocatalytic reduction of CO_2 on InP has not been reported with high efficiency.

In the work presented here, we investigate CO_2 reduction to CO by illuminating TiO_2-passivated InP with and without Pt nanoparticles in a nonaqueous ionic liquid solution. We investigate the role that ionic liquid [EMIM]BF_4 plays as a homogeneous catalyst for CO_2. The effects of the TiO_2 are explored by studying the photocurrent vs. reference potential characteristics systematically as a function of TiO_2 layer thickness. To our knowledge, this is the first report of photoelectrochemical reduction of CO_2 to CO by using a III–V compound semiconductor photocatalyst in an ionic liquid solution. The high Faradaic efficiencies achieved at substantial underpotential demonstrated the ability to drive CO_2 reduction efficiently using visible light.

Figure 1 shows the photocurrent-voltage curves for InP passivated with various thicknesses of TiO_2 measured in an AcN electrolyte with 0.02 M [EMIM]BF_4 under 532 nm illumination. At any given voltage, the TiO_2-passivated InP samples have a higher photocurrent than the bare InP (black curve). Under

[a] *G. Zeng, H. Shi, Prof. S. B. Cronin*
Department of Chemistry, University of Southern California
Los Angeles, California 90089
E-mail: scronin@usc.edu

[b] *J. Qiu*
Department of Materials Science, University of Southern California
Los Angeles, California 90089

[c] *B. Hou, Prof. S. B. Cronin*
Department of Electrical Engineering, University of Southern California
Los Angeles, California 90089

[d] *Dr. Y. Lin, M. Hettick, Prof. A. Javey*
Electrical Engineering & Computer Science Department
University of California, Berkeley, CA, 94720

Supporting information for this article is available on the WWW under http://dx.doi.org/10.1002/chem.201501671.

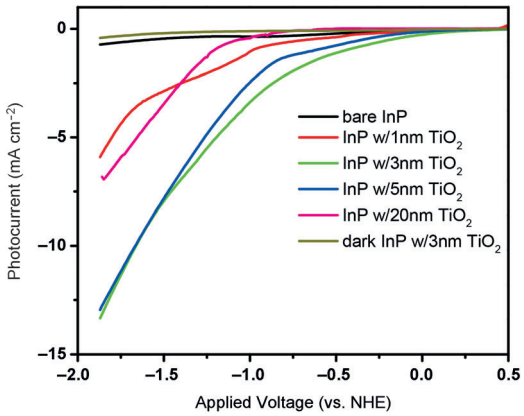

Figure 1. Photocatalytic current-potential curves of InP photocatalysts with different TiO_2 thicknesses in a 0.02 M [EMIM]BF_4 nonaqueous electrolyte, under 532 nm wavelength illumination.

an applied voltage of −1.37 V vs. NHE, we can see a clear improvement in the photocurrent of samples with TiO_2 passivation. From this data, we find that 3 nm thick TiO_2 produces the best conditions for photocatalysis. The trong dependence on TiO_2 thickness indicates there is a tradeoff between the benefits of the TiO_2 layer and its insulating nature, which eventually outweighs its benefits in thicker TiO_2 films (20 nm curve). Figure 1 also shows the current-potential characteristics of 3 nm TiO_2 passivated InP with and without laser illumination. This improvement observed with TiO_2 is attributed to an increased photovoltage produced at the *pn*-junction formed between the TiO_2 and InP. Here, the TiO_2 deposited by ALD is *n*-type due to oxygen vacancies and forms a *pn*-junction with the underlying *p*-type III–V compound photocathode.[18] This junction creates a built-in potential as well as band offsets between TiO_2 and InP that assist in the separation of photogenerated electron-hole pairs, and enables electrons to overcome the high barriers associated with this reaction through the associated increase in photovoltage produced at the junction.

Figure 2a shows the photocurrent-voltage curves for Pt nanoparticles deposited on various thicknesses of TiO_2-passivated InP measured in an AcN electrolyte with 0.02 M [EMIM]BF_4 under 532 nm illumination. The 1 nm TiO_2 film gives the highest photocurrent. However, the photocatalytic performance does not depend strongly on the TiO_2 thickness with the Pt co-catalyst. Figure 2b shows a comparison of the 1 nm TiO_2-passivated InP photocatalysts with and without Pt nanoparticles from Figure 1 and 2a, respectively. Here, the Pt co-catalyst increases the photocurrent by more than 25-fold at 0 V vs. NHE. There appears to be a synergistic effect between TiO_2 and Pt perhaps by the introduction of new active sites at the tri-phase boundary between the TiO_2, Pt, and electrolyte. The Pt co-catalyst provides enhancement in the photocatalytic reduction of CO_2 by extracting electrons from the semiconductor (TiO_2/InP), thus decreasing the probability of recombination with photogenerated holes, and enhancing charge transfer and surface binding of reactants in solution.[14]

Photoluminescence (PL) spectroscopy gives a relative measure of the nonradiative recombination in a material. Figure 3 shows the PL spectra of InP with various thicknesses of TiO_2 and with/without Pt nanoparticles (for each type of sample measured, several photoluminescence spectra were taken from different regions of the sample. These spectra were consistent within <1% variation). Here, the TiO_2 film reduces the PL intensity of InP by a factor of 2.5 (Figure 3a), and the Pt nanoparticles further reduce this by an additional factor of 2 (Figure 3b). This is likely due to the high density of surface states in the TiO_2, which act as nonradiative recombination centers,

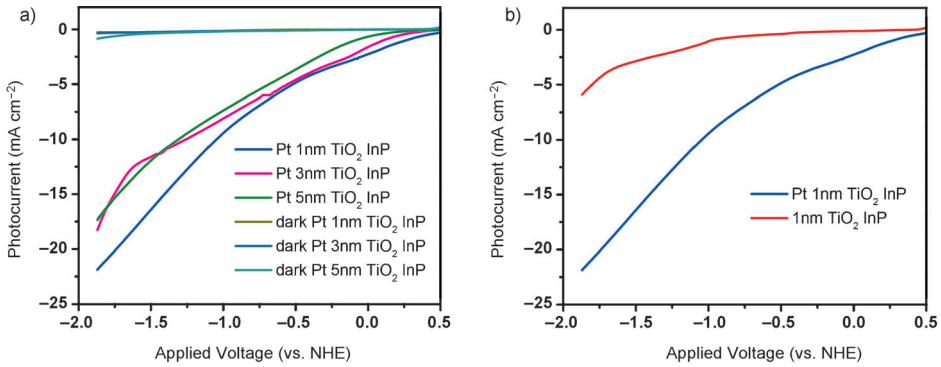

Figure 2. a) Photocatalytic current-potential curves of InP photocatalysts with Pt nanoparticles with various thicknesses of TiO_2 in a 0.02 M [EMIM]BF_4 non-aqueous electrolyte under 532 nm wavelength laser illumination. b) Photocurrent-potential curves of 1 nm TiO_2-passivated InP compared to 1 nm TiO_2-passivated InP with Pt nanoparticles.

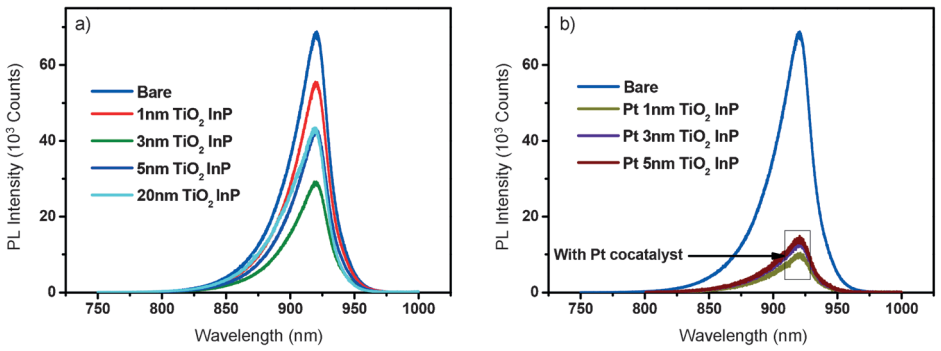

Figure 3. Photoluminescence spectra of a) InP passivated with various thickness of TiO_2. b) Pt nanoparticles deposited on TiO_2-passivated InP.

thus lowering the PL efficiency. So, contrary to what one might expect, the best photocatalyst has the lowest PL efficiency and vice versa. From this data, it is apparent that the TiO_2 films and their surface states cause strong electron-hole recombination; however, the benefit that they provide by lowering the potential barriers of the reaction and promoting charge transfer outweighs their detriment associated with charge recombination.

The role of the active surface states can be further confirmed by running the same reaction in $LiClO_4$ electrolyte, as shown previously by Ramesha et al.[19] Here, the small Li^+ cations bind strongly to the charged surface states essentially poisoning these sites, making them catalytically inactive.[20] Figure S1 of the Supporting Information shows the photo-*I*–*V* curves taken with and without the $LiClO_4$ electrolyte. From this data, it is clear that the CO_2 reduction reaction is blocked by the presence of the Li^+ ions, which demonstrates the importance of the catalytically active surface states, as previously shown by Ramesha et al.[21] As a comparison, the photo-*I*–*V* characteristics were obtained using $EMIM^+$ solution with N_2 gas instead of CO_2, as shown in Figure S1 (Supporting Information). The results obtained with CO_2 in the Li^+ solution closely resemble those taken with N_2, in which no photoreduction of CO_2 is possible. By contrast, when running the reaction without Li^+ ions in ionic liquid solution, the surface sites remain active and can catalyze the reduction of CO_2. Here, the $[EMIM]^+$ ions in the ionic liquid solution do not have the same poisoning effect since this is a larger molecule, unable to provide sufficient Coulombic screening of these active surface states.

The nonaqueous ionic liquid electrolyte is important for suppressing hydrogen evolution (i.e., water splitting), which has a much lower energy barrier. When illuminated, TiO_2-passivated InP produces CO as quantified by gas chromatography described in the Experimental Section below. Of all the samples without Pt nanoparticles measured in this study, the 3 nm TiO_2-passivated InP sample exhibits the highest CO Faradaic efficiency of 89% at −1.57 V (vs. NHE). This corresponds to an overpotential of just 0.02 V compared to the standard redox potential $E^\circ(CO_2/CO) = -1.55$ V (vs. NHE) in IL/AcN (see the calculation in the Supporting Information). The results of the gas analysis were consistent with the photo-*I*–*V* data, which also showed the 3 nm TiO_2-passivated sample to have the highest performance. We also observe CO_2 reduction at underpotentials of 0.18 and 0.68 V with Faradaic efficiencies of 50 and 39%, respectively, as listed in Table 1. For the samples with Pt co-catalyst, 1 nm TiO_2-passivated InP gives the best performance with 99% Faradaic efficiency at an underpotential of 0.78 V (−0.77 V vs. NHE), as listed in Table 1. Table S1 in the Supporting Information lists the Faradaic efficiencies of CO for various thicknesses of TiO_2-passivated InP in 0.02 M $[EMIM]BF_4$ ionic liquid electrolyte taken after 4 h of illumination with 532 nm wavelength light at an underpotential of 0.18 V.

Figure 4a shows the ^1H NMR spectrum of the reaction products after 4 h illumination of 3 nm TiO_2-passivated InP in $[EMIM]BF_4$, Figure 4b shows the ^1H NMR spectrum of pure $[EMIM]BF_4$. In Figure 4a, the main resonance lines in the spectrum correspond to the protons of the pure IL. The $[EMIM]BF_4$ ionic liquid was chosen for these experiments since CO_2 is known to form weak complexes with BF_4 anions, as compared with other ionic liquids. As reported by Rosen et al., the intermediate complex formed can be expressed as EMIM-CO_2*···BF_4, in which the intermediate EMIM-CO_2* is bonded weakly with BF_4^- ions. Ideally, this CO_2* complex is bound strongly enough to facilitate CO_2 reduction, but not too strongly as to render the CO_2* unreactive.[10] The formation of the bound EMIM-CO_2* intermediate compound, as previously established by Rosen and Sun, is evidenced by the low intensity set of peaks in the

Table 1. Photocatalytic conversion of CO_2 to CO on 3 nm TiO_2-passivated InP and 1 nm TiO_2-passivated InP with Pt nanoparticles in 0.02 M $[EMIM]BF_4$ in AcN electrolyte under 532 nm wavelength laser illumination.

Applied voltage [V][a]	Underpotential [V][b] 3 nm TiO_2 InP	CO Faradaic efficiency (%)
−1.57	−0.02	89 ± 5
−1.37	+0.18	50 ± 8
−0.87	+0.68	39 ± 10
1 nm TiO_2 InP with Pt nanoparticles		
−1.37	+0.18	98 ± 3
−1.17	+0.38	97 ± 6
−0.97	+0.58	98 ± 4
−0.77	+0.78	99 ± 3

[a] Applied potentials here are referenced vs. NHE. [b] Underpotentials are given with respect to the standard redox potential of $E^\circ = -1.55$ V (vs. NHE) in the ionic liquid solution.

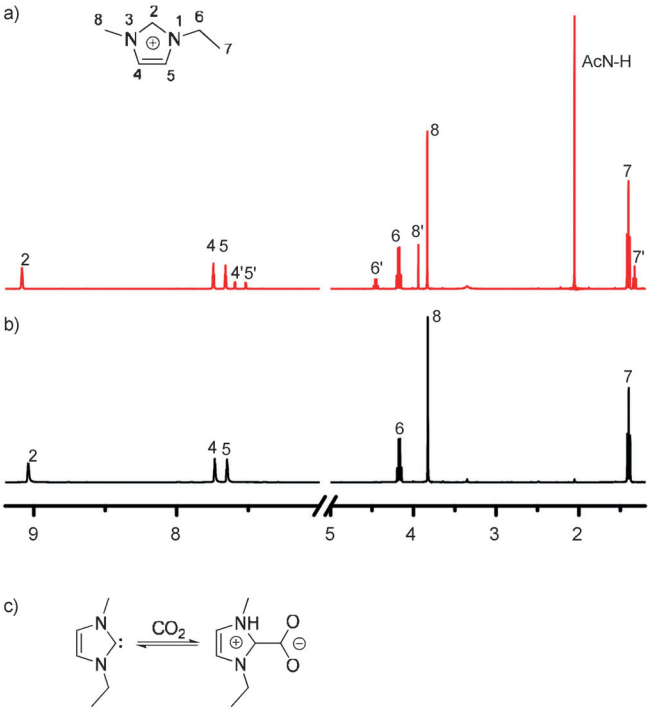

Figure 4. a) ^1H NMR spectrum (in DMSO, reference to TMS) of 0.02 M $[EMIM]BF_4$ electrolyte solution after 4 h of CO_2 reduction. b) ^1H NMR spectrum of pure $[EMIM]BF_4$. c) Schematic representation of the intermediate complex that is formed between the [EMIM] ion and the CO_2^-.

NMR spectrum of Figure 4a, which are labeled with prime symbols (e.g., 4′, 5′).[10,11] No resonant H peaks appear on C_2, which indicates that the CO_2 molecule is binding to the C_2 of the imidazolium ring to form the intermediate species, as illustrated in Figure 4c.

As a control experiment, we compared photocatalysis performed in the 0.02 M $[EMIM]BF_4$ in AcN electrolyte with that performed in a CO_2 saturated 0.5 M KCl (pH 7) aqueous electrolyte at −1.37 V (vs. NHE) under 532 nm irradiation. Here, we found that only hydrogen was produced in the aqueous solution, further establishing the importance of the non-aqueous electrolyte for CO_2 reduction reactions. Also, we ran the experiment at −1.37 V (vs. NHE) on 3 nm TiO_2-passivated InP without light irradiation and detected no CO. In order to rule out other possible sources of carbon in this reaction, we repeated the experiment by bubbling argon as the control gas instead of CO_2, and observed no CO_2 reduction products. We also ran the experiment using isotopically labeled $^{13}CO_2$, and observed ^{13}CO (molecular weight 29), as shown in Figure S2 in the Supporting Information, verifying that CO_2 is indeed the main carbon source in this reaction. Figure S3 in the Supporting Information plots the Faradaic efficiencies of the CO and carboxylate products as a function of $[EMIM]BF_4$ concentration in an AcN electrolyte under 532 nm wavelength illumination. From this data, it is clear that the molarity has little effect on the Faradaic efficiency of the products, and 0.02 M is sufficient to run the reaction.

These photocatalysts represent complex photoelectrochemical systems, and it is difficult to separate the physical (e.g., photovoltaic) and chemical (e.g., surface intermediates) processes in the overall efficiency. The main advantages of this system, compared to bulk TiO_2, are physical in nature. Namely, the band gap of InP is close to the optimum band gap derived in the Shockley–Queisser limit for solar utilization. Also, InP's carrier transport and lifetimes far exceed those of TiO_2. One nontrivial aspect of these photocatalysts is the low resistance Ohmic contact formatted on the back of the InP wafer, without which efficiencies would be considerably lower. On the chemical side, overpotential losses are reduced by the introduction of catalytically active sites and the formation of intermediate complexes.

In conclusion, we report photocatalytic CO_2 reduction to CO at high underpotentials on TiO_2-passivated InP with a Pt co-catalyst in a non-aqueous $[EMIM]BF_4$ ionic liquid electrolyte. The nonaqueous solution prohibits hydrogen formation and enables CO_2 reduction with a Faradaic efficiency of 99% at an underpotential of 0.78 V. The TiO_2 passivation layer provides enhancement in the photoconversion efficiency through the formation of a charge separating *pn*-region and active surface states, which reduces carrier recombination and lowers the external potential required to initiate this reaction. The TiO_2 layer reduces the photoluminescence intensity indicating that these active surface states cause electron-hole recombination; however, the benefits of the TiO_2 film outweigh its detriment associated with charge recombination. The Pt co-catalyst provides substantial enhancement in the Faradaic efficiency of this reaction system. NMR spectroscopy shows the formation of an intermediate complex $[EMIM\text{-}CO_2]^*$, which further lowers the energy of the reaction pathway.

Experimental Section

General

The non-aqueous solution was prepared using acetonitrile (AcN, 99.99%), DMSO (99.96% D, Sigma Aldrich), and $[EMIM]BF_4$ (99.0%, HPLC, Sigma Aldrich). An anion exchange membrane (Selemion AMV, Anion Exchange Membrane, AGC) was used to separate the working and counter electrodes to prevent the oxidation of reduced CO_2 products. This anion exchange membrane only allows negative ions to transfer through the membrane, which prevents the oxylate intermediate from participating in the oxygen evolution half-reaction at the counter electrode. *p*-type (100)-oriented InP with a Zn dopant concentration of 5×10^{17} cm^{-3} was used as the photocatalyst for CO_2 reduction with an active area of 0.5 cm × 1 cm. ALD of anatase TiO_2 was performed at 250 °C on the *p*-GaP wafers with $TiCl_4$ as the titanium source and water vapor as the oxygen source. Using ellipsometry, we established that 100 cycles of ALD produces a 4 nm-thick TiO_2 film and 1000 cycles produces a 40 nm film. Pt nanoparticles were deposited by electron beam evaporation with a nominal thickness of 0.8 nm. This is not thick enough to form a continuous film, and instead forms small islands or nanoparticles of Pt. XPS, plotted in Figure S6 of the Supporting Information, shows the presence of Ti^{3+} states, which are known to serve as catalytically active sites. The TEM image in Figure S7 (Supporting Information) shows that the TiO_2 films deposited on InP are amorphous in nature. A Zn–Au film was evaporated on the back of the *p*-InP to form an Ohmic contact. The Zn–Au contact was then connected to the external circuitry with a copper wire and coated with epoxy cement to insulate it from the electrolytic solution, as shown in Figure 5b.

A three-terminal potentiostat was used with the prepared semiconductor samples as the working electrode, a $Ag/AgNO_3$ reference electrode, and a Pt wire as the counter electrode, as shown in Figure 5a. The $Ag/AgNO_3$ electrode was made of a silver wire immersed in 0.01 M silver nitrate dissolved in 0.1 M TEAP/AcN. Also, the reference electrode was calibrated against a ferrocene/ferrocenium (Fc^+/Fc) redox couple to confirm that it gave the right potential with respect to NHE. Figure S5 (Supporting Information) shows this calibration curve. The potential applied between the reference and working electrodes was maintained by the potentiostat (Gamry, Inc.). Before each measurement, CO_2 was purged through the solution on the working electrode side of the electrochemical cell for 30 min to ensure a CO_2 saturated solution. In this setup, we analyzed the products evolving at the working electrode, instead of at the counter electrode. It is likely that oxygen is produced at the counter electrode in the reaction $4OH^- + 4e^+ \rightarrow O_2 + 2H_2O$. The gaseous products from the CO_2 reduction reaction were analyzed with a gas chromatograph (GC) (Bruker GC-450) equipped with a thermal conductivity detector (TCD) and a carbon-plot column (Agilent). A standard calibration curve was developed to quantify the CO yields from the photocatalytic surfaces, as shown in Figure S4 (Supporting Information). NMR spectroscopy was performed using a Varian spectrometer operating at 600 MHz. The samples were dried on a rotary evaporator at 40 °C under vacuum and then dissolved in DMSO. We observed only the CO product on the cathode side.

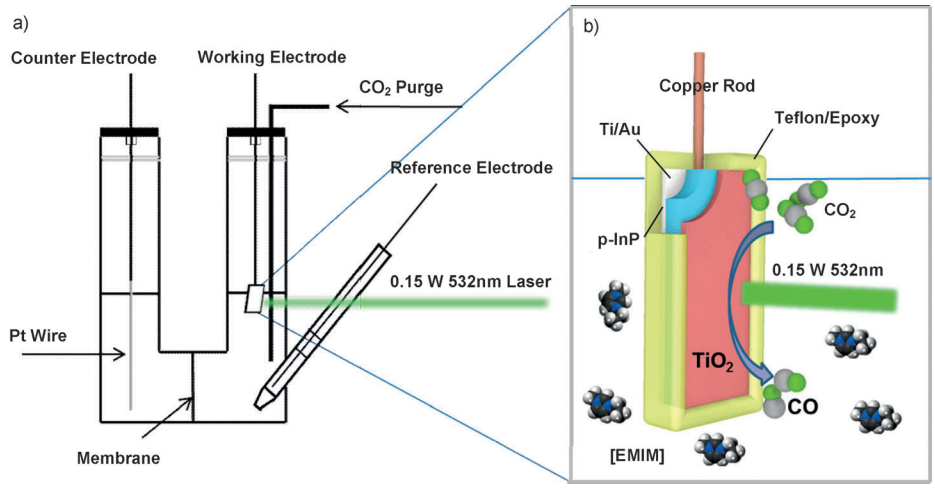

Figure 5. a) Schematic of the electrochemical cell. b) Sample geometry of TiO_2-passivated *p*-InP photocathode.

Acknowledgements

This research was supported by ARO award no. W911NF-14-1-0228 (J.Q.) and NSF award no. CBET-0846725 (G.Z.).

Keywords: CO_2 reduction · InP · ionic liquids · photochemistry · titanium

[1] a) M. Halmann, *Nature* **1978**, *275*, 115 – 116; b) T. Inoue, A. Fujishima, S. Konishi, K. Honda, *Nature* **1979**, *277*, 637 – 638.

[2] a) E. E. Benson, C. P. Kubiak, A. J. Sathrum, J. M. Smieja, *Chem. Soc. Rev.* **2009**, *38*, 89 – 99; b) B. Kumar, M. Llorente, J. Froehlich, T. Dang, A. Sathrum, C. P. Kubiak, *Annu. Rev. Phys. Chem.* **2012**, *63*, 541 – 569; c) C. Amatore, J. M. Saveant, *J. Am. Chem. Soc.* **1981**, *103*, 5021 – 5023; d) M. Cokoja, C. Bruckmeier, B. Rieger, W. A. Herrmann, F. E. Kühn, *Angew. Chem. Int. Ed.* **2011**, *50*, 8510 – 8537; *Angew. Chem.* **2011**, *123*, 8662 – 8690; e) C. Finn, S. Schnittger, L. J. Yellowlees, J. B. Love, *Chem. Commun.* **2012**, *48*, 1392 – 1399; f) A. Goeppert, M. Czaun, R. B. May, G. K. S. Prakash, G. A. Olah, S. R. Narayanan, *J. Am. Chem. Soc.* **2011**, *133*, 20164 – 20167; g) G. A. Olah, G. K. S. Prakash, A. Goeppert, *J. Am. Chem. Soc.* **2011**, *133*, 12881 – 12898; h) M. Le, M. Ren, Z. Zhang, P. T. Sprunger, R. L. Kurtz, J. C. Flake, *J. Electrochem. Soc.* **2011**, *158*, E45 – E49; i) A. J. Bard, L. R. Faulkner, *Electronchemical Methods*, **2001**, 2nd ed., p. 736; j) Y. Izumi, *Coord. Chem. Rev.* **2013**, *257*, 171 – 186; k) O. K. Varghese, MM. Paulose, T. J. LaTempa, C. A. Grimes, *Nano Lett.* **2009**, *9*, 731 – 737.

[3] G. Zeng, J. Qiu, Z. Li, P. Pavaskar, S. B. Cronin, *ACS Catal.* **2014**, *4*, 3512 – 3516.

[4] P. N. R. Vennestrøm, C. M. Osmundsen, C. H. Christensen, E. Taarning, *Angew. Chem. Int. Ed.* **2011**, *50*, 10502 – 10509; *Angew. Chem.* **2011**, *123*, 10686 – 10694.

[5] a) Z. Chen, C. Chen, D. R. Weinberg, P. Kang, J. J. Concepcion, D. P. Harrison, M. S. Brookhart, T. J. Meyer, *Chem. Commun.* **2011**, *47*, 12607 – 12609; b) A. J. Morris, G. J. Meyer, E. Fujita, *Acc. Chem. Res.* **2009**, *42*, 1983 – 1994; c) O. Jacquet, X. Frogneux, C. Das Neves Gomes, T. Cantat, *Chem. Sci.* **2013**, *4*, 2127 – 2131; d) C. Costentin, S. Drouet, M. Robert, J.-M. Savéant, *Science* **2012**, *338*, 90 – 94; e) C. Costentin, J. C. Canales, B. Haddou, J.-M. Savéant, *J. Am. Chem. Soc.* **2013**, *135*, 17671 – 17674; f) D. Canfield, K. W. Frese, *J. Electrochem. Soc.* **1983**, *130*, 1772 – 1773.

[6] I. Taniguchi, B. Aurian-Blajeni, J. O. M. Bockris, *Electrochim. Acta* **1984**, *29*, 923 – 932.

[7] a) K. Chandrasekaran, J. O. Bockris, *Surf. Sci.* **1987**, *185*, 495 – 514; b) J. O. Bockris, J. C. Wass, *J. Electrochem. Soc.* **1989**, *136*, 2521 – 2528; c) J. O. Bockris, J. C. Wass, *Mater. Chem. Phys.* **1989**, *22*, 249 – 280.

[8] a) G. Seshadri, C. Lin, A. B. Bocarsly, *J. Electroanal. Chem.* **1994**, *372*, 145 – 150; b) E. E. Barton, D. M. Rampulla, A. B. Bocarsly, *J. Am. Chem. Soc.* **2008**, *130*, 6342 – 6344.

[9] a) J. H. Koh, H. S. Jeon, M. S. Jee, E. B. Nursanto, H. Lee, Y. J. Hwang, B. K. Min, *J. Phys. Chem. C* **2015**, *119*, 883 – 889; b) L. L. Snuffin, L. W. Whaley, L. Yu, *J. Electrochem. Soc.* **2011**, *158*, F155 – F158.

[10] B. A. Rosen, A. Salehi-Khojin, M. R. Thorson, W. Zhu, D. T. Whipple, P. J. A. Kenis, R. I. Masel, *Science* **2011**, *334*, 643 – 644.

[11] L. Sun, G. K. Ramesha, P. V. Kamat, J. F. Brennecke, *Langmuir* **2014**, *30*, 6302 – 6308.

[12] a) J. L. DiMeglio, J. Rosenthal, *J. Am. Chem. Soc.* **2013**, *135*, 8798 – 8801; b) J. Medina-Ramos, R. C. Pupillo, T. P. Keane, J. L. DiMeglio, J. Rosenthal, *J. Am. Chem. Soc.* **2015**, *137*, 5021 – 5027; c) J. Medina-Ramos, J. L. DiMeglio, J. Rosenthal, *J. Am. Chem. Soc.* **2014**, *136*, 8361 – 8367.

[13] a) H. Yan, J. Yang, G. Ma, G. Wu, X. Zong, Z. Lei, J. Shi, C. Li, *J. Catal.* **2009**, *266*, 165 – 168; b) Q. Zhai, S. Xie, W. Fan, Q. Zhang, Y. Wang, W. Deng, Y. Wang, *Angew. Chem. Int. Ed.* **2013**, *52*, 5776 – 5779; *Angew. Chem.* **2013**, *125*, 5888 – 5891.

[14] S. Xie, Y. Wang, Q. Zhang, W. Deng, Y. Wang, *ACS Catal.* **2014**, *4*, 3644 – 3653.

[15] a) Y. Lin, R. Kapadia, J. Yang, M. Zheng, K. Chen, M. Hettick, X. Yin, C. Battaglia, I. D. Sharp, J. W. Ager, A. Javey, *J. Phys. Chem. C* **2015**, *119*, 2308 – 2313; b) S. Hu, M. R. Shaner, J. A. Beardslee, M. Lichterman, B. S. Brunschwig, N. S. Lewis, *Science* **2014**, *344*, 1005 – 1009; c) M. F. Lichterman, A. I. Carim, M. T. McDowell, S. Hu, H. B. Gray, B. S. Brunschwig, N. S. Lewis, *Energy Environ. Sci.* **2014**, *7*, 3334 – 3337; d) Y. W. Chen, J. D. Prange, S. Dühnen, Y. Park, M. Gunji, C. E. D. Chidsey, P. C. McIntyre, *Nat. Mater.* **2011**, *10*, 539 – 544.

[16] E. Aharon-Shalom, A. Heller, *J. Electrochem. Soc.* **1982**, *129*, 2865 – 2866.

[17] M. H. Lee, K. Takei, J. J. Zhang, R. Kapadia, M. Zheng, Y. Z. Chen, J. Nah, T. S. Matthews, Y. L. Chueh, J. W. Ager, A. Javey, *Angew. Chem. Int. Ed.* **2012**, *51*, 10760 – 10764; *Angew. Chem.* **2012**, *124*, 10918 – 10922.

[18] a) B. J. Morgan, G. W. Watson, *J. Phys. Chem. C* **2010**, *114*, 2321 – 2328; b) J. Qiu, G. Zeng, P. Pavaskar, Z. Li, S. B. Cronin, *Phys. Chem. Chem. Phys.* **2014**, *16*, 3115 – 3121.

[19] G. K. Ramesha, J. F. Brennecke, P. V. Kamat, *ACS Catal.* **2014**, *4*, 3249 – 3254.

[20] a) M. Anpo, H. Yamashita, Y. Ichihashi, S. Ehara, *J. Electroanal. Chem.* **1995**, *396*, 21 – 26; b) J. M. Pan, B. Maschhoff, U. Diebold, T. Madey, *J. Vac. Sci. Technol. A* **1992**, *10*, 2470 – 2476; c) G. Lu, A. Linsebigler, J. T. Yates Jr, *J. Phys. Chem.* **1994**, *98*, 11733 – 11738.

[21] B. H. Meekins, P. V. Kamat, *ACS Nano* **2009**, *3*, 3437 – 3446.

Received: May 6, 2015
Published online on ■■ ■■, 0000

COMMUNICATION

Efficiency and selectivity: Substantial improvements (up to 18×) in the photocatalytic yields for CO_2 reduction to CO through the surface passivation of InP with TiO_2 deposited by atomic layer deposition (ALD) is reported. Photoelectrochemical reactions were carried out in a nonaqueous solution consisting of ionic liquid 1-ethyl-3-methylimidazolium tetrafluoroborate ([EMIM]BF_4) dissolved in acetonitrile (see figure).

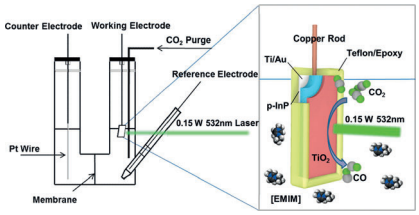

Solar Cells

*G. Zeng, J. Qiu, B. Hou, H. Shi, Y. Lin, M. Hettick, A. Javey, S. B. Cronin**

■■ – ■■

Enhanced Photocatalytic Reduction of CO_2 to CO through TiO_2 Passivation of InP in Ionic Liquids

Green Chemistry

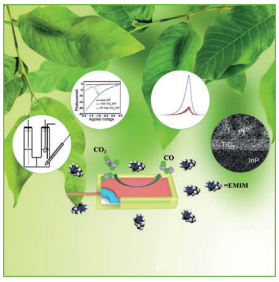

Photocatalytic reduction of CO_2 is an exciting reaction system with the ability to convert an abundant greenhouse gas to combustible hydrocarbon fuels using sunlight. In their Communication on page ■■ ff., S. Cronin et al. describe a robust and reliable method for improving the photocatalytic performance of InP, which is one of the best known materials for solar photoconversion. Substantial improvements (up to 18×) in the photocatalytic yields for CO_2 reduction to CO through the surface passivation of InP with TiO_2 deposited by atomic layer deposition (ALD) are reported.